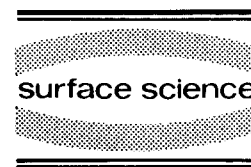




ELSEVIER

Surface Science 307-309 (1994) 704-709



# Adsorption of xenon on metals: a theoretical analysis

R. Pérez<sup>\*, a</sup>, F.J. García-Vidal<sup>a</sup>, P.L. de Andrés<sup>b</sup>, F. Flores<sup>a</sup>

<sup>a</sup> Departamento de Física de la Materia Condensada (C-XII), Facultad de Ciencias,  
Universidad Autónoma de Madrid, E-28049 Madrid, Spain

<sup>b</sup> Instituto de Ciencia de Materiales (CSIC), E-28006 Madrid, Spain

(Received 20 August 1993)

## Abstract

We present *free parameter* LCAO calculations for the adsorption of xenon on metal surfaces. This calculation yields the short-range interaction between the adatom and the surface for different adsorption sites. Our approach shows that the chemical interaction between the Xe orbitals and Al accounts for as much as half the adsorption energy, and consequently cannot be neglected. To deduce the total adsorption energy, we add the long-range van der Waals interaction calculated using a standard available theory for metals.

## 1. Introduction

Although the long-range van der Waals interaction is well understood at distances greater than hundreds of ångströms [1], we are still lacking a detailed understanding for smaller distances relevant to the problem of physisorption [2]. This fact has motivated in recent years a number of different approaches to understand the weak adsorption on surfaces. We cannot make an exhaustive survey of these here, but we should mention the original perturbative approach due to Zaremba and Kohn [3], the scattering formalism due to Chizmeshya and Zaremba [4,5], and the local density approach due to Lang [6]. The first two approaches share in common their attempt to describe the physisorption well using a repulsive interaction acting at very short distances due to the mutual repulsion of the electronic clouds and cores, and an attractive force due to the van der Waals interaction, given asymptotically by

$$V_{\text{pol}} \approx -\frac{C_3}{(z - z_{\text{vdW}})^3}, \quad (1)$$

where terms of order  $z^{-5}$  have been dropped and  $z_{\text{vdW}}$  is the reference plane where the expression diverges [5,7,8]. The LDA approach is radically different because, although the repulsive part has a similar physical origin, the attractive part comes mainly from the lowering in energy for the exchange and correlation hole located in high electronic density regions appearing between the metal surface and the adsorbate. Moreover, the local approximation precludes the correct asymptotic dependence, gives at long distances an exponential decay and produces a measurable disagreement between theory and experiment, as seen, for example, in the calculated sequence of bound state energies for the diffraction of helium. At the moment, it is not completely understood why an LDA theory is able to reproduce acceptably well the known details of the physisorption well [6] for Ar on Ag and the dipole moments for Xe on Al.

\* Corresponding author.

In this paper, we propose a new description of the weak adsorption of rare gases on metal surfaces following closely the method we have previously developed for the adsorption problem [9,10]. In addition to different contributions to the short-range energy found in our method, we include the asymptotic form for the potential represented by Eq. (1) and calculated using the work of other researchers [7,8,11]. Within this first-principles formalism we should be able to study a number of trends of interest, like adsorption energies for different positions on a given surface (and then, accurate surface diffusion barriers), the changes in adsorption for a series of different surfaces, and for a series of metals and/or different rare-gas atoms. Any of these problems is of sufficient interest to understand the accuracy of the theoretical description for the physisorption potentials, and we shall only mention recent attempts to determine the actual adsorption position for xenon deposited on platinum or nickel surfaces [12,13], or the activity to explain the known trends in physisorption of xenon on different faces of Pd [14,15].

In this work we shall concentrate on the weak adsorption of xenon on Al(100) [16], which is simple enough because it can be described only with s and p orbitals, but still retaining the important physics that will surely appear in the more complex transition metals.

## 2. Formalism

We use the LCAO method to calculate the short-range interaction between Xe and the metal. Long-range interactions can be described by a van der Waals potential, and we get this contribution to the binding energy from other authors [3,4]. Thus, our total Xe–metal potential will be given by the following equation:

$$V_t = V_{sr} + V_{vdw}, \quad (2)$$

where  $V_{sr}$  is the short-range Xe–metal potential.

Basically, our approach describes the Xe–metal interaction as a superposition of the different “bonds” defined for each pair of Xe–metal orbitals [17]:

$$\begin{aligned} \hat{H} = & \sum_{i,\sigma} E_i^\sigma \hat{n}_{i\sigma} + \sum_{\sigma,(i,j)} T_{ij}^\sigma (\hat{c}_{i\sigma}^\dagger \hat{c}_{j\sigma} + \hat{c}_{j\sigma}^\dagger \hat{c}_{i\sigma}) \\ & + \sum_i U_i \hat{n}_{i\uparrow} \hat{n}_{i\downarrow} + \frac{1}{2} \sum_{i,j \neq i,\sigma} [J_{ij} \hat{n}_{i\sigma} \hat{n}_{j\bar{\sigma}} \\ & + (J_{ij} - J_{x,ij} + J_{ij} S_{ij}^2) \hat{n}_{i\sigma} \hat{n}_{j\sigma}] \\ & + \sum_i \frac{Z_i Z_j}{d}, \end{aligned} \quad (3)$$

where

$$E_i = \epsilon_i + \sum_j [-S_{ij} T_{ij} + \frac{1}{4} S_{ij}^2 (\epsilon_i - \epsilon_j)]. \quad (4)$$

$T_{ij}$  is related to the Bardeen tunnelling current between atomic orbitals  $\phi_i$  and  $\phi_j$ ,  $U_i$  and  $J_{ij}$  being the different Coulomb interactions associated with the same atomic orbitals;  $J_{x,ij}$  defines the corresponding exchange interaction. The Hamiltonian (3) is obtained by expanding the full Xe–metal Hamiltonian up to a second order in the orbitals overlap  $S_{ij} = \langle \phi_i | \phi_j \rangle$ .

In Eq. (4),  $\epsilon_i$  is the  $i$ th atomic level and the terms  $[-S_{ij} T_{ij} + \frac{1}{4} S_{ij}^2 (\epsilon_i - \epsilon_j)]$  are associated with the repulsive kinetic energy appearing when two orbitals,  $i$  and  $j$ , start to overlap. These terms play a crucial role in describing the repulsive energy between the occupied Xe levels and the conduction metal orbitals. This can easily be understood by considering the simple case of a fully occupied Xe level (say, a sp orbital),  $E_1$ , interacting with a partially occupied level of the metal,  $E_2$ . One can prove [9] that for this case  $T_{12} \approx -\frac{1}{2} S_{12} (E_2 - E_1)$ , then the repulsive terms and the hybridization terms,  $T_{12}^2 / (E_1 - E_2)$ , associated with the hopping integral  $T_{12}$ , yield the following shifts in the Xe and metal levels:

$$\begin{aligned} \delta E_1 &= 0, \\ \delta E_2 &= S_{12}^2 (E_2 - E_1). \end{aligned} \quad (5)$$

This shift in the metal level measures the contribution of the one-electron terms to the repulsive potential between the occupied Xe orbitals and the metal. The total interaction is obtained by adding to that repulsion the Coulomb and exchange interaction associated with the many-body terms of the Hamiltonian (3).

The interaction of the empty 6s level of Xe with the metal is different. For close Xe–metal distances, the 6s level suffers an important hybridization and a slight electron charge can be transferred from the metal to the 6s level. This means that the Xe 6s wavefunction undergoes a chemisorption interaction with the substrate, then the Hamiltonian (3) has to be fully analyzed including the many-body terms associated with the electron–electron interaction.

Following Kohn and Sham, we introduce [17] the following local potential

$$V_{i\sigma}^{\text{mb}} = \frac{\partial E^{\text{mb}}[n_{i\sigma}]}{\partial n_{i\sigma}}, \quad (6)$$

where  $n_{i\sigma}$  is the  $i\sigma$  orbital occupancy, and  $E^{\text{mb}}$  the many-body energy of the ground state of the system.

The Hartree energy,  $E^{\text{H}}$ , is given by

$$E^{\text{H}} = \sum_i U_i n_{i\uparrow} n_{i\downarrow} + \frac{1}{2} \sum_{i,j \neq i,\sigma} [J_{ij} n_{i\sigma} n_{j\sigma} + \tilde{J}_{ij} n_{i\sigma} n_{j\sigma}] \quad (7)$$

and the exchange–correlation contribution can be written as

$$E^{\text{xc}} = -\frac{1}{2} \sum_{i,\sigma} \tilde{J}_i n_{i\sigma} (1 - n_{i\sigma}), \quad (8)$$

where  $\tilde{J}_i$  is an average interaction between the  $n_{i\sigma}$  charge and its exchange–correlation hole  $(1 - n_{i\sigma})$ . Notice that Eq. (8) defines the following exchange–correlation potential:

$$V_{i\sigma}^{\text{xc}} = -\tilde{J}_i \left(\frac{1}{2} - n_{i\sigma}\right) \quad (9)$$

for the almost empty Xe 6s level,  $n_{i\sigma} \approx 0$ , and  $V_{i\sigma}^{\text{xc}}$  describes the image potential that lowers that level towards the metal Fermi energy.

Our analysis of the Xe 6s level interacting with the metal is based on the solution of the Hamiltonian (3), using the many-body terms that are treated in a local-density approach by means of Eqs. (6)–(9).

In summary, the short-range interaction between Xe and the metal is given by the superposition of two different contributions: (i) First of all, we find the repulsive potential between

the Xe occupied levels and the metal. This interaction is mainly a repulsive kinetic energy associated with the overlap between the Xe and metal orbitals. (ii) The second important contribution between Xe and the metal is associated with the empty Xe 6s level. Here, some electron-charge transfer appears, and the interaction has a chemisorptive character instead of the physisorptive one appearing in the previous case. The analysis of this case has to be done by considering fully the many-body terms of the Hamiltonian (3) that yield an important contribution to the total “chemisorption” energy.

### 3. Results

We present detailed results for the physisorption of xenon on Al(100). In our calculations, the metal surface is described by using conventional tight-binding parameters [19]. The method described above has been applied to the calculation of the xenon–metal interaction. The atomic wavefunctions used to obtain the different parameters of the Hamiltonian (3) have been taken from atomic tables [20] or calculated from standard atomic calculations (this is the case for the xenon 6s level) [21]. We have analyzed the cases of xenon approaching the metal surface along different directions: centre, bridge and top sites.

Fig. 1 shows the short-range xenon–metal interaction for the centre and the top sites as a function of the metal–atom distance measured from the last metal layer. In the same figure we also show the van der Waals interaction calculated using Eq. (1) with the parameters given in Ref. [5]. The total energy is obtained by adding the short- and long-range interactions: a minimum is obtained for distances around 8.7 a.u., with a binding energy of 177 and 157 meV for the centre and top positions, respectively (the bridge binding energy being around 165 meV). In order to understand the different contributions to the short-range interaction, we show in Fig. 2 this energy split into its different constituents: (a) kinetic repulsion; (b) electrostatic; (c) hybridization and (d) many-body energies. It is interest-

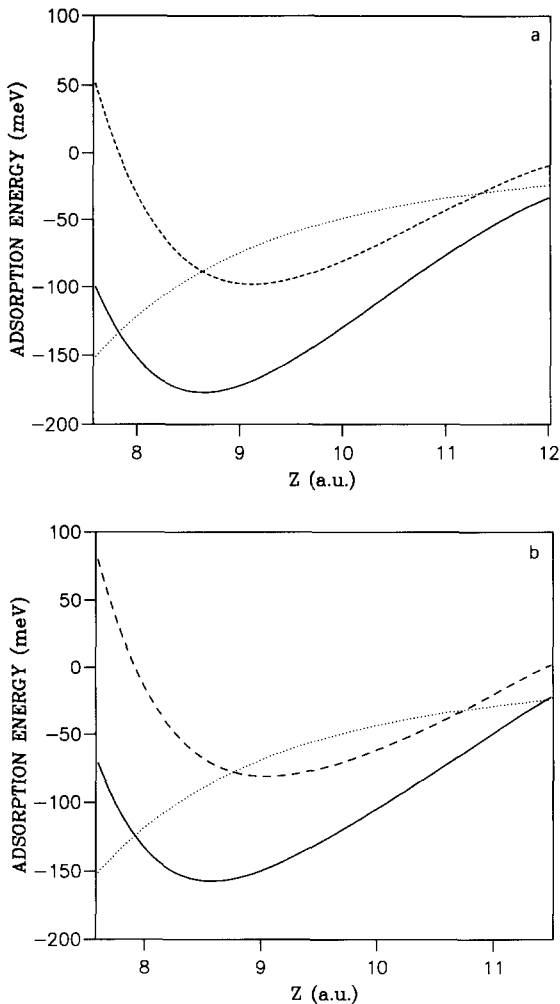


Fig. 1. Adsorption potentials for Xe/Al(100) for the centre (a) and top (b) positions. Broken lines represent the short-range contribution to the potential, dotted lines the van der Waals long-range part and the full line the whole potential.

ing to realize that the short-range interaction is very repulsive as long as the metal–xenon distance gets smaller than 8.0 a.u.: this is mainly due to the high repulsive kinetic energy associated with the large overlap between the occupied levels of xenon and the metal wavefunctions. The high electron metal density of aluminium yields this large metal–xenon overlap when the rare-gas atom tries to penetrate the metal, increasing very efficiently the metal–xenon repulsion.

On the other hand, we find an attractive short-

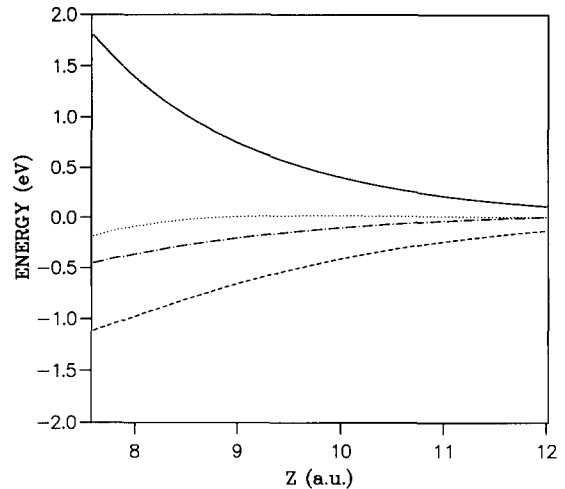


Fig. 2. Different terms contributing to the short-range interaction between the xenon and the aluminium surface in the centre position: kinetic repulsive (full line); electrostatic (dotted line); hybridization (broken line) and many-body energies (broken dotted line).

range interaction for metal–xenon distances larger than 8.5 a.u. This effect is mainly due to the hybridization and the many-body effects that overcome the kinetic energy repulsion. This is a typical chemisorption effect associated with the hopping between the xenon 6s level and the metal: some charge transfer is induced from the metal to the xenon due to the 6s broadening (about 0.1 electrons) and the hybridization and many-body terms increase relative to the kinetic energy repulsion.

The short-range interaction between xenon and aluminium can be understood in the following way: (i) at distances between 8.5 and 10 a.u., the potential is dominated by the xenon 6s level that defines a weak chemical interaction with the metal substrate. This explains the attractive short-range potentials found in Fig. 1 for the centre and on top positions; (ii) at distances smaller than 8.0 a.u. the repulsion associated with the xenon occupied levels (5p orbitals and other inner shells) starts to dominate and the xenon atom is not allowed to penetrate the metal.

It is also interesting to understand the differences found in Fig. 1 for the centre and on top

positions, with a slightly larger binding short-range energy for the centre one. Basically, the differences are related to larger hopping integrals appearing between xenon and the metal for the centre position. The interplay between the number of nearest neighbours defining basically the bonds and, their respective distance determine, in a complex way, the hybridization and exchange and correlation energies, favouring slightly the centre position for the present case.

Finally, it is also worth remarking that for the xenon–aluminium interaction, we find that the total binding energy, around 177 meV, is almost equally split into its short- and long-range contributions. Moreover, our results show a small barrier,  $\sim 20$  meV, for the motion of the atom in the direction parallel to the surface. We remark that these results are in good agreement with the experimental evidence (experimental binding energies being around 200 meV [16]) and other LDA calculations [18].

#### 4. Conclusions

Our results for the xenon–aluminium interaction show that the short-range potential plays an important role, contributing as much as half of the value for the total binding energy. We have shown that this is basically due to a chemical interaction between the xenon 6s level and the metal, that in the past has not received too much attention, except using qualitative models [22]. Furthermore, we remark that this interaction is also selecting the centre site as the favoured adsorption position. The other ingredient yielding the equilibrium xenon–metal distance is associated with the strong repulsion between the filled xenon levels and the high aluminium electron density: this is created by the highly repulsive kinetic energy due to the overlap between occupied levels.

How can this picture be extended to transition metals? We have explored the case of xenon interacting with the Ni(100) surface. Our preliminary results give a strong indication of a new relevant physical picture in this case. The nickel

metal has a conduction band with s–p bond and d electrons: the s–p electrons control the xenon–metal interaction at distances larger than approximately 7 a.u. However, the picture is now different from the aluminium case: the main reason is that the s–p metal electron density is smaller than the one found for aluminum, and both the xenon 6s level and the inner shells interact more weakly with the metal. This implies that: (i) First of all, the short-range interaction for distances larger than 8 a.u. is not any more attractive; on the contrary, we find a slightly repulsive potential due to the weak interaction of the xenon 6s level with the metal. (ii) Second, the xenon inner shells and the metal also have a weaker repulsion. All these effects tend to weaken the xenon–metal interaction, allowing the xenon to penetrate the metal to shorter distances. Eventually, this effect brings the metal d levels to the balance, and makes the equilibrium nickel–xenon distance much shorter than the aluminium–xenon one.

In conclusion, our LCAO analysis allows us to show the different effects operating in the metal–xenon interaction. In particular, we should stress that the chemical reactivity between the s–p levels of aluminium and the 6s level of xenon is very important for explaining the total binding energies. Preliminary results show that for nickel (and likely for other transition metals), the d electrons play an important role due to the weak interaction between the metal sp electrons and different xenon orbitals.

#### Acknowledgements

This research was supported in part by the CICYT under Contracts Nos. PB92-0168 and PB91-0930. Support by the CEE (SCI-CT-91-0691) is gratefully acknowledged. F.F. also acknowledges financial help by Iberdrola S.A.

#### References

- [1] V. Sandoghdar, C.I. Sukenik and E.A. Hinds, *Phys. Rev. Lett.* 68 (1992) 3432.

- [2] A. Zangwill, *Physics at Surfaces* (Cambridge University Press, Cambridge, 1988).
- [3] E. Zaremba and W. Kohn, *Phys. Rev. B* 13 (1976) 2270.
- [4] A. Chizmeshya and E. Zaremba, *Surf. Sci.* 268 (1992) 432.
- [5] A. Chizmeshya and E. Zaremba, *Surf. Sci.* 220 (1989) 443.
- [6] N.D. Lang, *Phys. Rev. Lett.* 46 (1981) 842.
- [7] A. Liebsch, *Phys. Rev. B* 36 (1987) 7378.
- [8] B.N.J. Persson and E. Zaremba, *Phys. Rev. B* 30 (1984) 5669.
- [9] E.C. Goldberg, A. Martin-Rodero, R. Monreal and F. Flores, *Phys. Rev. B* 39 (1989) 5684.
- [10] F.J. Garcia-Vidal, A. Martin-Rodero, F. Flores, J. Ortega and R. Perez, *Phys. Rev. B* 44 (1991) 11412.
- [11] C. Schwartz and R.J. Le Roy, *Surf. Sci.* 166 (1986) L141.
- [12] J.E. Muller, *Phys. Rev. Lett.* 65 (1990) 3021.
- [13] P.S. Weiss and D.M. Eigler, *Phys. Rev. Lett.* 69 (1992) 2240.
- [14] K. Wandelt and J.E. Hulse, *J. Chem. Phys.* 80 (1984) 1340.
- [15] C. Girard and C. Girardet, *Phys. Rev. B* 36 (1987) 909.
- [16] U. Scheider, G.R. Castro, H. Isern, T. Janssens and K. Wandelt, *Surf. Sci.* 251/252 (1991) 551.
- [17] F.J. García-Vidal, R. Pérez, J. Ortega and F. Flores, to be published.
- [18] A. Baratoff, S. Ciraci and E. Stoll, 14.43 Communication to the 13th General Conference of the Condensed Matter Division, European Physical Society.
- [19] D.A. Papaconstantopoulos, *Handbook of the Band Structure of Elemental Solids* (Plenum, New York, 1986).
- [20] E. Clementi and C. Roetti, *At. Data Nucl. Data Tables* 14 (1974) 177.
- [21] S.G. Louie, S. Froyen and M.L. Cohen, *Phys. Rev. B* 26 (1982) 1738.
- [22] K. Wandelt and B. Gumhalter, *Surf. Sci.* 140 (1984) 355.